

# Surface wettability of silicon substrates enhanced by laser ablation

Shih-Feng Tseng · Wen-Tse Hsiao · Ming-Fei Chen ·  
Kuo-Cheng Huang · Sheng-Yi Hsiao · Yung-Sheng Lin ·  
Chang-Pin Chou

Received: 19 November 2009 / Accepted: 10 May 2010 / Published online: 16 June 2010  
© Springer-Verlag 2010

**Abstract** Laser-ablation techniques have been widely applied for removing material from a solid surface using a laser-beam irradiating apparatus. This paper presents a surface-texturing technique to create rough patterns on a silicon substrate using a pulsed Nd:YAG laser system. The different degrees of microstructure and surface roughness were adjusted by the laser fluence and laser pulse duration. A scanning electron microscope (SEM) and a 3D confocal laser-scanning microscope are used to measure the surface micrograph and roughness of the patterns, respectively. The contact angle variations between droplets on the textured surface were measured using an FTA 188 video contact angle analyzer. The results indicate that increasing the values of laser fluence and laser pulse duration pushes more molten slag piled around these patterns to create micro-sized craters and leads to an increase in the crater height and surface roughness. A typical example of a droplet on a laser-textured surface shows that the droplet spreads very quickly

and almost disappears within 0.5167 s, compared to a contact angle of 47.9° on an untextured surface. This processing technique can also be applied to fabricating Si solar panels to increase the absorption efficiency of light.

## 1 Introduction

Wettability is an important characteristic of solid surfaces, and is usually measured by the contact angle between water and the surface. If the contact angle is less than 90°, the surface is hydrophilic; if it is greater than 90°, the surface is hydrophobic, and if it is greater than 150°, the surface is superhydrophobic. The chemical composition and microscopic geometric structure of the surface also determines its wettability: the higher the free energy is, the higher the wettability, and vice-versa. In general, a solid surface becomes hydrophobic when treated to give micro- or nano-roughness structures and low surface energy. Many kinds of surface treatment techniques, including optical micro-lithography, dry and wet etching, surface coating and precision diamond dicing processes were reported [1–4]. To reduce the production costs and increase the processing speeds, current laser micro- or nano-machining processes employ techniques such as laser ablation, laser milling, and laser deposition. These techniques have been effectively used to manufacture components with enhanced hydrophobic properties [5, 6].

In this research, a laser-ablated technique has been used to create rough patterns on a silicon substrate to enhance the surface wettability. The effect of several parameters, such as the laser fluence and laser pulse duration are explored using an Nd:YAG laser source. After laser ablation of silicon substrates, a scanning electron microscope (SEM) and a 3D laser-scanning microscope are used to measure the

S.-F. Tseng (✉) · W.-T. Hsiao · K.-C. Huang · S.-Y. Hsiao  
Instrument Technology Research Center, National Applied  
Research Laboratories, Hsinchu 30076, Taiwan  
e-mail: [tsengsf@itrc.org.tw](mailto:tsengsf@itrc.org.tw)  
Fax: +886-3-5773947

S.-F. Tseng · C.-P. Chou  
Department of Mechanical Engineering, National Chiao Tung  
University, Hsinchu 30010, Taiwan

M.-F. Chen  
Department of Mechatronics Engineering, National Changhua  
University of Education, Changhua 50058, Taiwan

Y.-S. Lin  
Department of Applied Cosmetology & Graduate Institute  
of Cosmetic Science, Hungkuang University, Taichung 43302,  
Taiwan

surface micrograph and roughness of the rough patterns, respectively. The contact angle variations between droplets on the textured surface were measured using a surface tension analyzer.

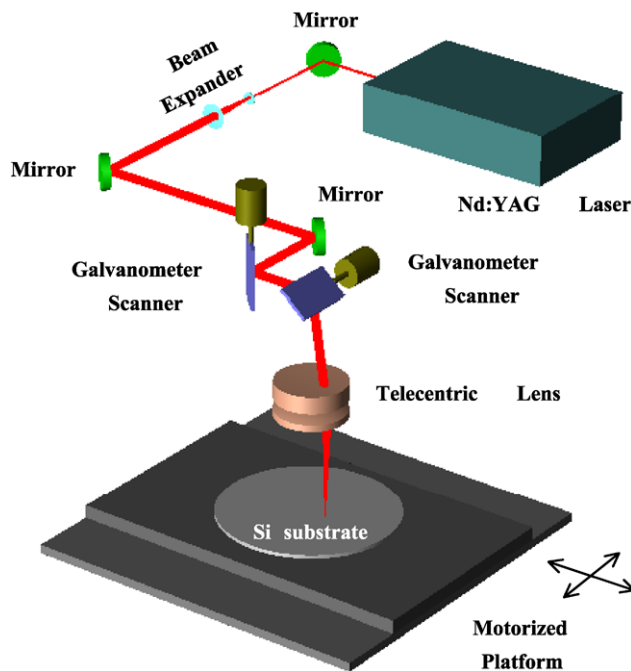


**Fig. 1** Schematic diagram of the Nd:YAG laser set-up

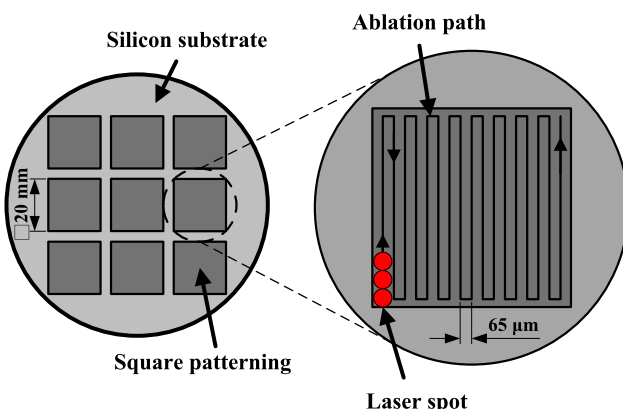
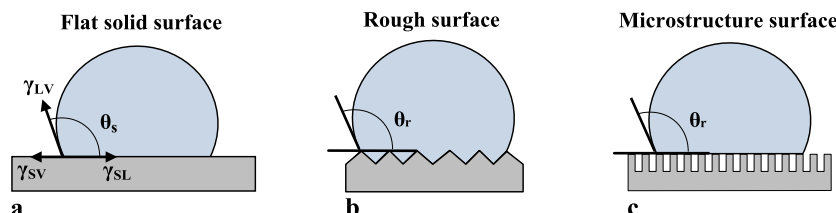


**Fig. 2** The illustration of laser-ablation path

**Fig. 3** Cross-sectional view of the droplet on target surfaces



## 2 Experimental

### 2.1 Apparatus and sample

The current experimental studies focus on surface texturing created in silicon substrates using a diode-pumped, Q-switched Nd:YAG laser system (Optowave model Awave-IR). Figure 1 shows a schematic diagram of the experimental set-up used to fabricate rough-patterned templates. A laser beam via three reflective mirrors, a beam expander, two galvanometer scanners, and a telecentric lens is focused on the experimental surface. The nominal laser-beam diameter at the exit port and average spot size are 0.8 mm and 30  $\mu\text{m}$ , respectively. The laser is emitted at the fundamental wavelength of 1064 nm, the maximum laser average power is approximately 20 W, and pulse repetition rate ranges from 20 kHz to 100 kHz. The laser pulse width is ranging from 34 to 76 ns. Additionally, the commercial silicon plates with single-face polished were chosen as substrates. The substrate is 500  $\mu\text{m}$  thick and 100 mm in diameter.

Characterization measurements were performed with the following techniques and instrumentations: The surface micrograph and roughness patterns were measured using a SEM and a 3D confocal laser-scanning microscope (VK-9700, KEYENCE Corp.) with 0.1 nm resolution of vertical and horizontal measured range, respectively. The laser power was monitored with a Gentec Electro-Optics SOLO 2 laser power meter. The light reflection rate of the silicon substrate was measured using a spectrophotometer system (LAMBDA 900). Droplet characteristics, such as the contact angle, size, and shape were measured with an FTA 188 video contact angle analyzer.

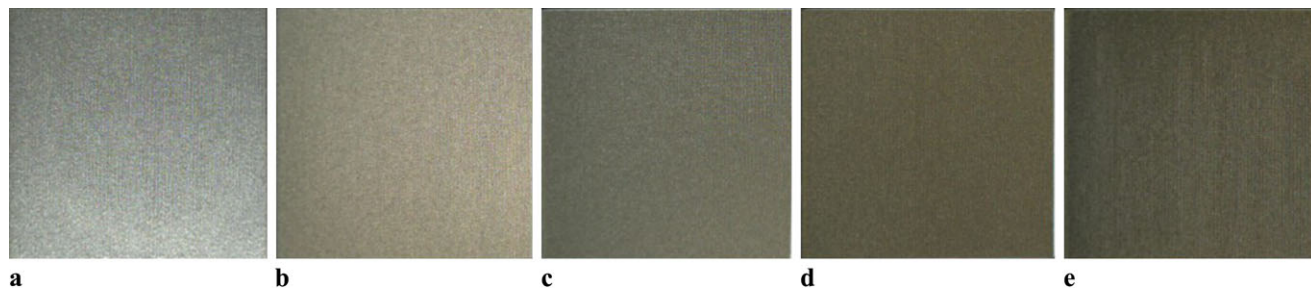
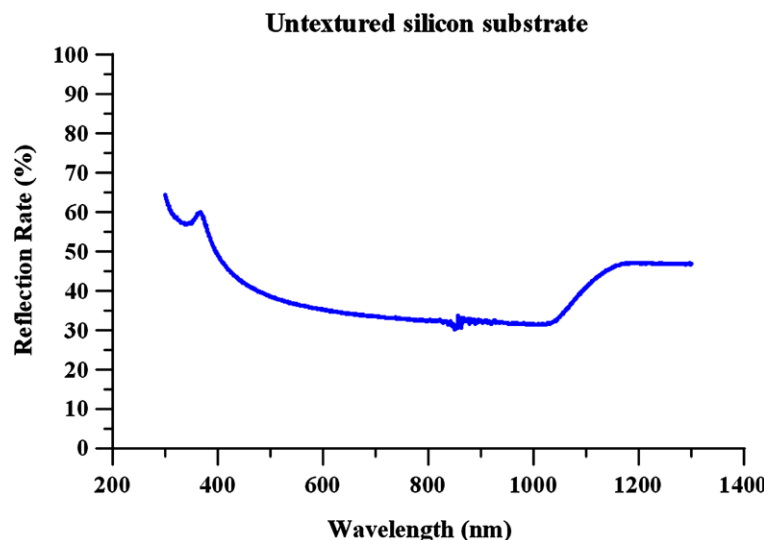
### 2.2 Surface texturing by laser ablation

Figure 2 shows the laser-ablation path of parallel lines with equal scan spacing. The dimensions of ablated area and ablated pitch are 20 mm  $\times$  20 mm and 65  $\mu\text{m}$ , respectively. In addition, the experimental parameters including laser fluence ( $F$ ) and laser pulse duration ( $Pd$ ) were adjusted to create patterns of different roughness via a PC-based controller.

### 2.3 Wettability characteristics of the textured surfaces

Droplet experiments were carried out to describe the wettability behavior of the textured surfaces used in this research. A droplet volume of 3  $\mu\text{L}$  was gently placed on the

**Fig. 4** Optical characteristics of untextured silicon substrate



**Fig. 5** Some examples for laser-ablated squares on silicon substrate under different test parameters. (a)  $F = 49.5 \text{ J/cm}^2$ ,  $Pd = 100 \mu\text{s}$ , (b)  $F = 53.8 \text{ J/cm}^2$ ,  $Pd = 100 \mu\text{s}$ , (c)  $F = 11.8 \text{ J/cm}^2$ ,  $Pd = 300 \mu\text{s}$ , (d)  $F = 53.8 \text{ J/cm}^2$ ,  $Pd = 300 \mu\text{s}$ , (e)  $F = 53.8 \text{ J/cm}^2$ ,  $Pd = 500 \mu\text{s}$

**Fig. 6** SEM micrographs showing the effect of laser pulse duration on surface structures at  $F = 53.8 \text{ J/cm}^2$ :  
(a)  $Pd = 100 \mu\text{s}$ ,  
(b)  $Pd = 300 \mu\text{s}$ ,  
(c)  $Pd = 500 \mu\text{s}$

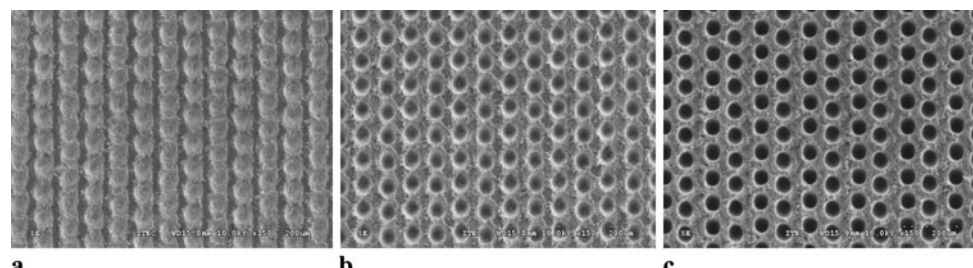


**Fig. 7** SEM micrographs showing the effect of laser fluence on surface structures at  $Pd = 300 \mu\text{s}$ :  
(a)  $F = 17.1 \text{ J/cm}^2$ ,  
(b)  $F = 29.1 \text{ J/cm}^2$ ,  
(c)  $F = 37.5 \text{ J/cm}^2$

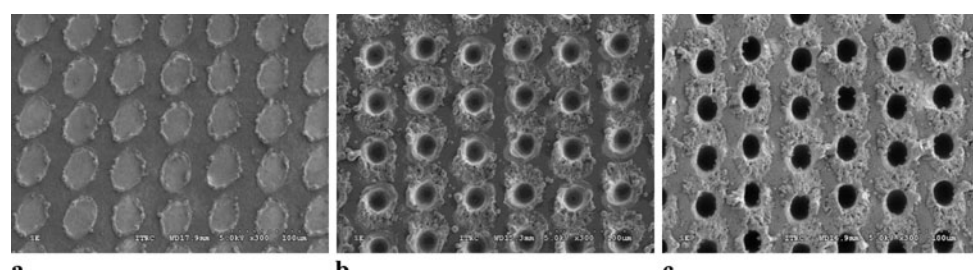
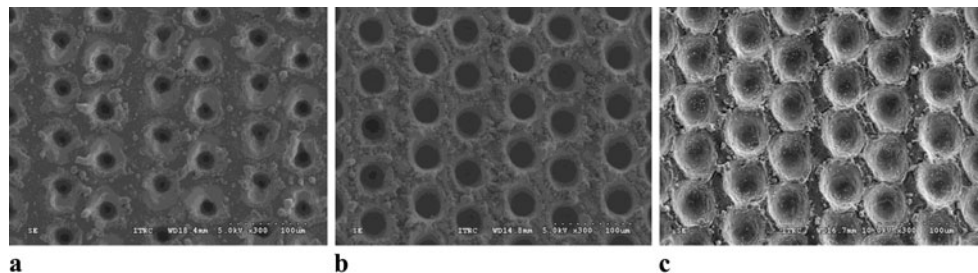


**Fig. 8** SEM micrographs showing the effect of laser fluence on surface structures at  $P_d = 500 \mu\text{s}$ :  
**(a)**  $F = 29.1 \text{ J/cm}^2$ ,  
**(b)**  $F = 42.1 \text{ J/cm}^2$ ,  
**(c)**  $F = 92 \text{ J/cm}^2$



textured surfaces in these experiments using a micropipette and droplet shapes were captured to measure the apparent contact angle by a FTA 188 video contact angle analyzer. A cross-sectional view of the droplet on three types of target surfaces is shown in Fig. 3. From Fig. 3(a), a contact angle  $\theta_s$  of a liquid droplet on a flat solid surface is given by the classical Young equation:

$$\cos \theta_s = \frac{\gamma_{SV} - \gamma_{SL}}{\gamma_{LV}} \quad (1)$$

where  $\gamma_{SV}$ ,  $\gamma_{LV}$ , and  $\gamma_{SL}$  are the interfacial free energies per unit area of the solid–vapor, liquid–vapor, and solid–liquid interfaces, respectively. The Young's equation describes wetting on an ideal surface, i.e., a smooth and chemically homogeneous surface at equilibrium. As for the rough surface of Fig. 3(b), Wenzel [7] proposed a theoretical model describing the contact angle,  $\theta_r$ , by modifying (1) as follows:

$$\cos \theta_r = \frac{r(\gamma_{SV} - \gamma_{SL})}{\gamma_{LV}} = r \cos \theta_s \quad (2)$$

where  $r$  is the roughness factor defined as the ratio of the actual area of a rough surface to the geometric projected area. Because this factor is always larger than 1, the surface roughness enhances the hydrophilicity of hydrophilic surfaces and also enhances the hydrophobicity of hydrophobic ones. The liquid droplet is the only contact with the top side of the microstructures, as shown in Fig. 3(c). Cassie and Baxter [8] described this condition and the contact angle  $\theta_r$  for the microstructure surface using (3):

$$\cos \theta_r = \phi(\cos \theta_s + 1) - 1 \quad (3)$$

where  $\phi$  is the fraction of the solid–liquid interface below the drop. Equations (2) and (3) only consider droplets on a single morphological surface. Textured surfaces, however, often have complex morphologies that result in different surface energy configurations by laser processes. Therefore, the characteristics of liquid droplets related to the surface roughness and the microstructure were investigated.

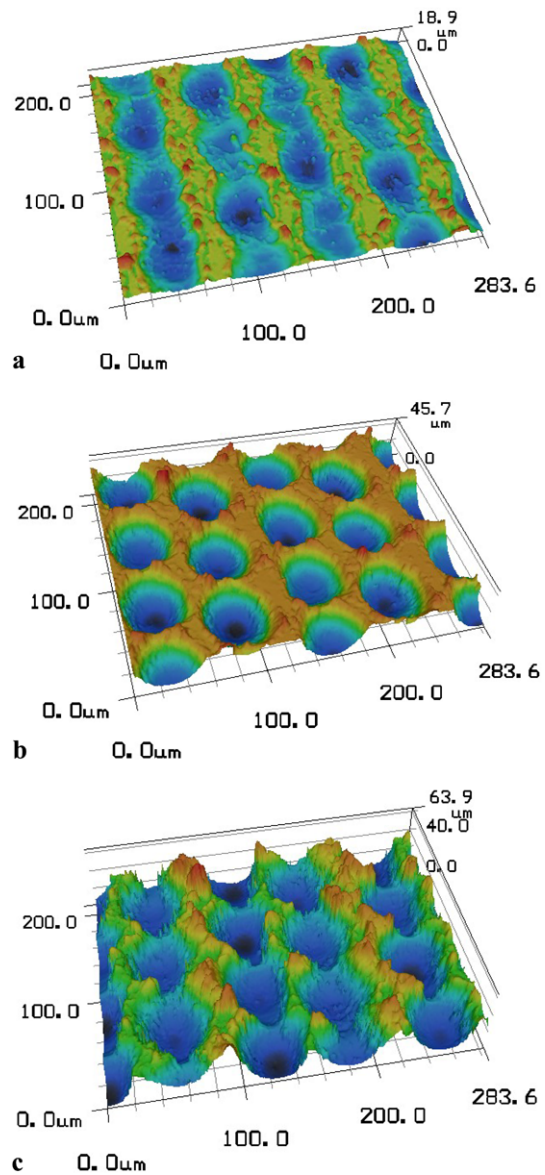


**Fig. 9** Typical 3D confocal laser-scanning microscope topographies of texture formed on silicon surface at  $F = 70.7 \text{ J/cm}^2$ :  
**(a)**  $P_d = 100 \mu\text{s}$ , **(b)**  $P_d = 300 \mu\text{s}$ , **(c)**  $P_d = 500 \mu\text{s}$

### 3 Results and discussion

#### 3.1 Square patterning on silicon substrates

Figure 4 shows the light reflection rate of the untextured silicon substrate before the laser ablation, using a spectrophotometer system to measure the optical characteristics of the silicon substrate. The reflection rate is 32.5% for the Nd:YAG laser (1064 nm) wave band. The value of absorptivity ( $A$ ) varies with the reflectivity ( $R$ ). For opaque materials, the absorption rate can be calculated as  $A = 1 - R$ . Thus, the absorption rate of the untextured silicon substrate is 67.5%. The laser-ablated samples with square patterning under different test parameters are shown in Fig. 5. These images show the color change by different thermal effects on the textured surface.

##### 3.1.1 Surface morphologies

In this study, the designed image was  $400 \times 400$  pixels from a .bmp file translation for square patterning on silicon substrates; each bit size and scan spacing is about  $65 \mu\text{m}$ . After laser texturing was carried out on the silicon substrates, the surface morphologies of the microstructures produced by pulses with  $F$  ranging from  $17.1$  to  $92 \text{ J/cm}^2$  were analyzed using an SEM. Figure 6 shows the SEM micrographs at  $150\times$  magnification, demonstrating the effect of  $Pd$  on the surface structures for  $F = 53.8 \text{ J/cm}^2$  and various  $Pd$  values of  $100 \mu\text{s}$  (a),  $300 \mu\text{s}$  (b), and  $500 \mu\text{s}$  (c), respectively. By increasing  $Pd$ , honeycombed structures with deeper holes are formed on the textured surface, as shown in Fig. 6(c). However, by decreasing these values, the laser spots are linked together and a structure with shallow grooves is formed (Fig. 6(a)). Figures 7 and 8 show a series of SEM micrographs at  $300\times$  magnification, demonstrating the effect of various  $F$  values on the surface structures for  $Pd$  values of  $300 \mu\text{s}$  and  $500 \mu\text{s}$ , respectively. By increasing the value

of  $F$ , honeycombed structures with deeper and bigger holes are formed on the textured surface, and more molten slag is piled around these holes to create micro-sized craters. Figure 9 shows typical 3D topographies of textures formed at  $1000\times$  magnification on silicon surfaces for  $F = 70.7 \text{ J/cm}^2$  and various  $Pd$  values. The ablated volume of each maximum crater height was calculated using a 3D confocal laser-scanning microscope analyzer, and the crater heights increased from  $18.6 \mu\text{m}$  (a) to  $45.7 \mu\text{m}$  (b) to and  $63.9 \mu\text{m}$  (c) as the  $Pd$  were increased to  $100 \mu\text{s}$ ,  $300 \mu\text{s}$ , and  $500 \mu\text{s}$ , respectively. Therefore, it appears that increasing  $Pd$  pushes the molten silicon outward and increases the crater height.

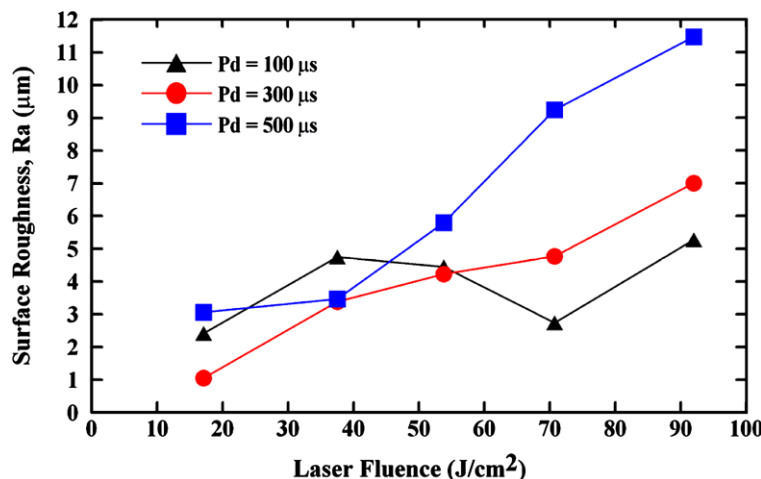
##### 3.1.2 Surface roughness

Figure 10 shows the effect of the laser fluence on the surface roughness measured using the 3D confocal laser-scanning microscope with a measuring region of  $200 \times 200 \mu\text{m}^2$ , for different test conditions. The results show that the surface roughness gradually increases with increasing  $Pd$  and demonstrate that the laser fluence has a strong effect on the surface roughness. This trend is similar to the results reported in the femtosecond laser micromilling of Si wafers [9] and in UV laser ablation of InP surfaces [10].

#### 3.2 Enhanced wettability of liquid droplets on laser-textured surfaces

After laser ablation of the silicon substrates, these surfaces exhibited complex morphologies and roughness that resulted in different surface energy configurations. Figure 11 displays typical image sequences of spreading liquid droplets on an untextured surface and a laser-textured surface with parameters of  $F = 53.8 \text{ J/cm}^2$  and  $Pd = 500 \mu\text{s}$ . According to (2), the surface roughness enhances the hydrophilicity of hydrophilic surfaces and enhances the hydrophobicity of hydrophobic ones. Thus, the results show

**Fig. 10** The effect of the laser fluence on the surface roughness for different conditions



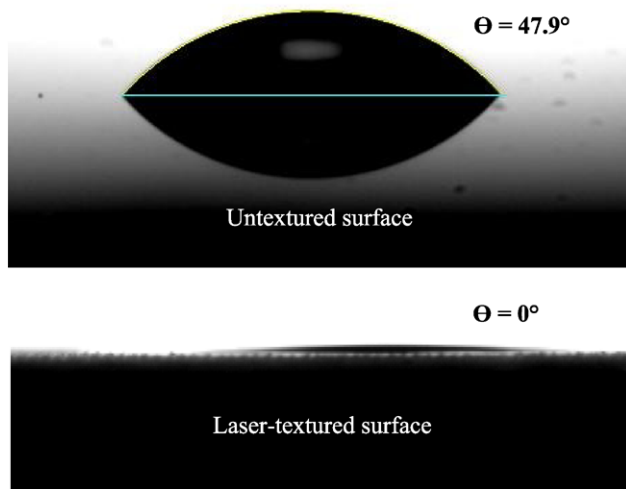


**Fig. 11** Comparison with images of spreading liquid droplets on untextured and laser-textured surfaces within 0.516 s

that the water droplet spreads very quickly and almost disappears within 0.5167 s on a laser-textured surface, compared to a contact angle of  $47.9^\circ$  on an untextured surface.

#### 4 Conclusions

This research has successfully demonstrated that the use of laser ablation to create rough patterns on a silicon substrate. Experimental parameters such as laser fluence and laser pulse duration were discussed. Using an SEM and a 3D confocal laser-scanning microscope, the surface micrograph and roughnesses of the textured substrates were observed. By increasing the laser fluence and laser pulse duration during laser ablation, more molten slag was piled around the

formed holes to create micro-sized craters and the crater height and surface roughness also increased. However, decreasing these parameters caused the laser spots to link together and a structure with shallow grooves was formed on the textured surface with decreased crater height and surface roughness. A typical example of placing a 3  $\mu\text{L}$  droplet on the laser-textured surface showed that the droplet spread very quickly and almost disappeared within 0.5167 s, compared to a contact angle of  $47.9^\circ$  on an untextured surface. In the future, this processing technique can also be used to fabricate Si solar panels to increase the absorption efficiency of light.

**Acknowledgements** The authors would like to thank the National Science Council of the Republic of China, Taiwan for financially/partially supporting this research under Contract No. NSC 98-2221-E-492-008.

#### References

1. Z. Yoshimitsu, A. Nakajima, T. Watanabe, K. Hashimoto, *Langmuir* **18**, 5818 (2002)
2. J. Lee, B. He, N.A. Patankar, *J. Micromech. Microeng.* **15**, 591 (2005)
3. H. Schulz, M. Leonhardt, H.-J. Scheibe, B. Schultrich, *Surf. Coat. Technol.* **200**, 1123 (2005)
4. M. Miwa, A. Nakajima, A. Fujishima, K. Hashimoto, T. Watanabe, *Langmuir* **16**, 5754 (2000)
5. R. Kannan, D. Sivakumar, *Colloids Surf. A* **317**, 694 (2008)
6. M. Groenendijk, *Laser Technol. J.* **3**, 44 (2008)
7. R.N. Wenzel, *J. Ind. Eng. Chem.* **28**, 988 (1936)
8. A.B.C. Cassie, S. Baxter, *Trans. Faraday Soc.* **40**, 546 (1944)
9. S. Lee, D. Yang, S. Nikumb, *Appl. Surf. Sci.* **254**, 2996 (2008)
10. O.R. Musaev, O.S. Kwon, J.M. Wrobel, D.-M. Zhu, M.B. Kruger, *Appl. Surf. Sci.* **254**, 5803 (2008)